International Journal of Fluid Machinery and Systems
Vol. 5, No. 3, July-September 2012
DOI:http://dx.doi.org/ 10.5293/IJFMS.2012.5.3.134
ISSN (Online): 1882-9554

Original Paper

Experimental and computational analysis of behavior of three-way catalytic converter under axial and radial flow conditions.

Arif Zakaria Taibani [1] and Vilas Kalamkar [2]

[1] PG student, Thermal Engineering, Bharati Vidya Bhavan's, Sardar Patel College of Engineering, Mumbai 400058, India.
[2] Associate professor, Department of Mechanical Engineering, Bharati Vidya Bhavan's, Sardar Patel College of Engineering, Mumbai 400058, India.

Abstract

The competition to deliver ultra-low emitting vehicles at a reasonable cost is driving the automotive industry to invest significant manpower and test laboratory resources in the design optimization of increasingly complex exhaust after-treatment systems. Optimization can no longer be based on traditional approaches, which are intensive in hardware use and laboratory testing. The CFD is in high demand for the analysis and design in order to reduce developing cost and time consuming in experiments. This paper describes the development of a comprehensive practical model based on experiments for simulating the performance of automotive three-way catalytic converters, which are employed to reduce engine exhaust emissions. An experiment is conducted to measure species concentrations before and after catalytic converter for different loads on engine. The model simulates the emission system behavior by using an exhaust system heat conservation and catalyst chemical kinetic sub-model. CFD simulation is used to study the performance of automotive catalytic converter. The substrate is modeled as a porous media in FLUENT and the standard k-e model is used for turbulence. The flow pattern is changed from axial to radial by changing the substrate model inside the catalytic converter and the flow distribution and the conversion efficiency of CO, HC and NOx are achieved first, and the predictions are in good agreement with the experimental measurements. It is found that the conversion from axial to radial flow makes the catalytic converter more efficient. These studies help to understand better the performance of the catalytic converter in order to optimize the converter design.

Keywords: Catalyst, CFD modeling, chemical reaction, conversion efficiency, simulation.

1. Introduction

Most of the cities have a large number of automobiles; as a consequence they suffer from problems of air pollution. People of all ages can be affected from air pollution and particularly from sources, such as vehicle exhausts and residential heating, but mainly those with existing heart and respiratory problems are in an extra risk. Considering all the above, it can be concluded that transport has a great impact on the atmospheric environment and therefore it is necessary to reduce emissions from the road traffic.

The need to control engine emissions was recognized as early as 1909. Due to the more stringent rules and emission standards, automotive manufacturers begun to develop a treatment device for exhaust gases known as catalytic converter for their vehicle models. General Motors was the pioneer in the early 1970s followed by Ford and Chrysler. Catalytic converters came in many concepts, structures and even the materials; nevertheless, it continued to evolve depending on different vehicle requirements. Gasoline and diesel fuels are mixtures of hydrocarbon, compounds that contain hydrogen and carbon atoms. In a perfect engine, oxygen in the air would convert all the hydrogen in the fuel to water and all the carbon in the fuel to carbon dioxide. In reality, the combustion process cannot be perfect and automotive engines emit several types of pollutants. Ideally, when the ratio of the fuel and air is stoichiometric, the combustion of fuel in air will proceed to full completion. The products of such an ideal combustion process consists only carbon dioxide, water and nitrogen. In reality, in the product there are unburned fuel, nitrogen oxide and carbon monoxide along with carbon dioxide and water.

Catalytic converters are emission-control devices that have been used in passenger automobiles since 1975. The function of a catalytic converter is to chemically change harmful pollutants that the engine has combusted in the process of its various starting, driving, power and idle conditions. Catalytic converters were developed and adopted for automobile use because of rising concerns over smog and other harmful car emissions.

Received October 18 2011; revised August 4 2012; accepted for publication August 18 2012: Review conducted by Prof. Youn-Jae Kim. (Paper number O11022K).
Corresponding author: Arif Z. Taibani, PG Student, arif_zakaria@yahoo.com

Figure 1 shows the schematic diagram of catalytic converter. The catalytic converter consists of a core or substrate, washcoat and catalyst. . The core is often a ceramic honeycomb in modern catalytic converters, but stainless steel foil honeycombs are also used. A washcoat is used to make converters more efficient, often as a mixture of silica and alumina. The catalyst itself is most often a precious metal. Catalyst is a term in chemistry for a substance that promotes a chemical reaction without itself being affected. Platinum is the most active catalyst and is widely used. Platinum and rhodium are used as a reduction catalyst, while platinum and palladium are used as an oxidization catalyst.

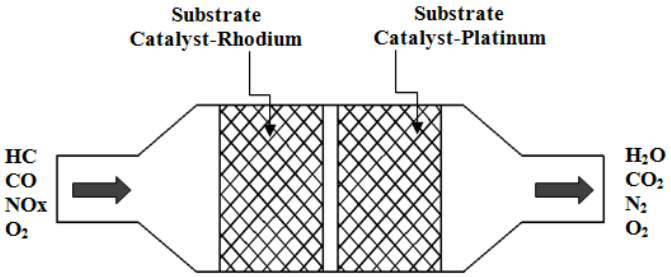

Fig. 1 Schematic diagram of Three-way Catalytic converter.

2. Reaction Scheme

The reduction catalyst is the first stage of the catalytic converter. It uses rhodium to reduce the NO_x emissions. When an NO or NO_2 molecule contacts the catalyst, the catalyst rips the nitrogen atom out of the molecule and holds on to it, freeing the oxygen in the form of O_2. The oxidation catalyst is the second stage of the catalytic converter. It reduces the unburned hydrocarbons and carbon monoxide by oxidizing them over a platinum and palladium catalyst. The third stage of conversion is a control system that monitors the exhaust stream, and uses this information to control the fuel injection system. The chemical reactions are adopted in this paper is:

1: $$2NO \rightarrow N_2 + O_2$$

2: $$2NO_2 \rightarrow N_2 + 2O_2$$

3: $$2CO + O_2 \rightarrow 2CO_2$$

4: $$C_xH_y + \left(\frac{x+y}{2}\right)O_2 \rightarrow xCO_2 + \frac{y}{2}H_2O$$

3. Radial flow catalytic converter

Figure 2 shows schematic of radial flow catalytic converter in which flow enters radially in the substrate which results in the optimal fluid dynamics and increase in conversion efficiency. The radial flow model allows very high cell densities and completely even distribution of the exhaust gas to the cell.

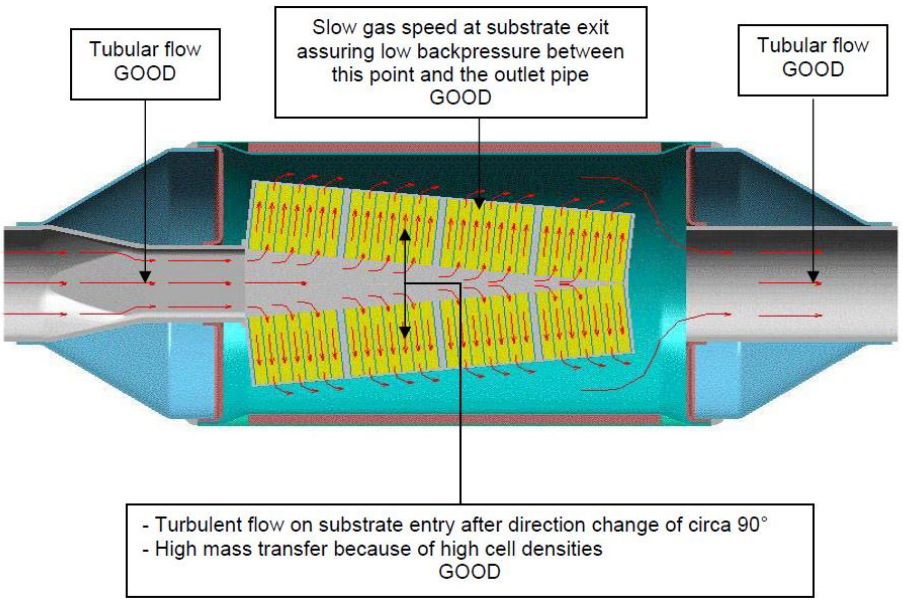

Fig. 2 Schematic diagram of radial flow catalytic converter.

4. Experimental Analysis

The measurements of engine catalyst system behavior, species concentrations and conversion efficiencies were performed on an engine catalyst setup. Figure 3 shows the instrumental setup used in the experiment.

4.1. Engine and dynamometer:

A Maruti Alto 796cc engine is used in the experiment. The engine was a modern 3 cylinder, 4 stroke petrol (MPFI), water cooled engine. The engine is coupled to a eddy current absorbing type dynamometer. The dynamometer worked at constant speed mode (1200 rpm); and the stepper motor controlled the load to the targeted value. The readings are taken at 0%, 50% and 80% load.

4.2. Catalytic converter:

The three way catalytic converter is used in the experiment. The catalytic converter has two brick setup. The front bricks are loaded with palladium and rear bricks with platinum and rhodium. Each brick is 100 cm in diameter and 70 cm in length and have square cells.

4.3. Instrumentations:

A KM9106EM Quintox emissions analyzer is used for the measurements of exhaust gas concentrations, which is supplied by Kane international limited. The concentrations of CO, HC, NO_x, CO_2, and O_2 are recorded before and after catalytic converter using this analyzer. The recorded concentrations are compared with the simulated results. The temperature at various points is measured using thermometer and thermocouple. The thermocouples placed at various locations of exhaust pipe and catalytic converter.

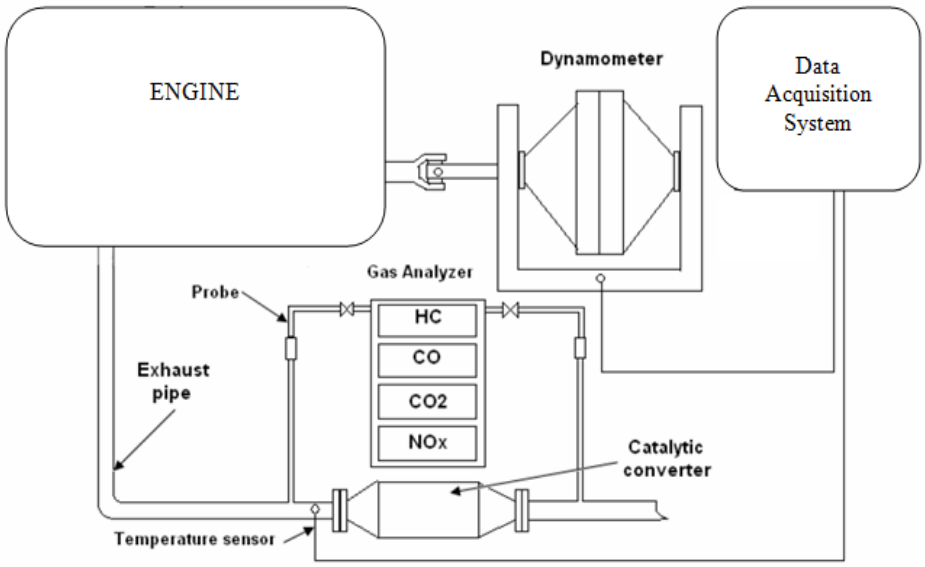

Fig. 3 Experimental setup

Table 1 Experimental measurement of species concentration before catalytic converter.

Load (KW)	SO_2 (ppm)	NO_2 (ppm)	NO (ppm)	CO_2 (%)	CO (%)	HC (ppm)	Temp (^oC)
0	24	43	117	4.2	0.157	36	161
2	9	223	317	8.6	0.465	255	247
4	0	530	600	17.9	1.14	700	347

Table 2 Experimental measurement of species concentration after catalytic converter.

Load (KW)	SO_2 (ppm)	NO_2 (ppm)	NO (ppm)	CO_2 (%)	CO (%)	HC (ppm)	Temp (^oC)
0	5	-	76	4.9	0.093	28	84
2	0	18	56	10.1	0.115	43	162
4	0	11	28	20.32	0.142	60	277

5. Computational Analysis

The 1D catalyst modeling has been around since the late 1960s with Vardi and Biller's [1] work among the first reported. Their work was very similar to pipe wall models examining only the effects of heat transfer on the warm-up of a catalyst. A few years later, Kuo et al [2] simulated a catalytic converter using a series of completely mixed reactors. In this work, they expanded the model to include exothermic/endothermic reactions on the surface as well as the propagation of chemical species throughout the device. Harned [3] later revised the reactor model to better represent the flow through a monolithic device while also adding a film model representing species on the surface of the catalyst. The models of Kuo et al. and Harned survived relatively intact until Oh and Cavendish [4] decided to examine the kinetic expressions in more detail. Specifically, they separated out the catalytic surface area term from the geometric surface area term to take into account its effect on chemical kinetics. A number of years later, Pattas et al. [5] added another equation for the surface chemistry to take into account surface intermediate chemistry. These classical models have been in widespread use and proven their effectiveness in designing catalyst. S. Siemund, D. Schweich [12] and T. Shamim [13] modeled a three way catalytic converter and compared the simulated results with the experimental measurements. Few years later, Depcik C. [16] considered a modeling of recting gases and after treatment devices for internal combustion engines. Recently, Niu Xiaowei and Zhang He [19] considered a effect of monolith wall thickness on the light off performance of a catalytic converter. This paper describes the 3D modeling of three way catalytic converter with flow distribution and chemical reactions.

5.1. Model description

The 3D three-way catalytic converter model is created in ICEM-CFD. Heated exhaust gas enters through the inlet of an exhaust manifold, passes through the runner and enters the substrate inside the catalytic converter. The substrate is modeled as a porous media in FLUENT, where viscous and inertial losses are specified in both the stream-wise and transverse directions. The flow is turbulent at the inlet and outlet whereas laminar in the substrate. By using the porous media model, the number of cells in the computational mesh can be reduced significantly, since the small geometric details of the substrate do not need to be resolved. After passing through the catalytic converter, the gas exits through the tail pipe. The realizable k-e model is used for turbulence, along with the standard wall function treatment. The fluid is assumed to be incompressible. Due to the varying complexity of the geometry, a hybrid mesh is chosen to minimize the preprocessing time. Tetrahedral cells are utilized in the exhaust runners, substrate and tail pipe. A velocity inlet boundary condition is used at the inlet and a constant pressure boundary condition is prescribed at the tail-pipe exit. The species concentrations at the inlet measured in the experiment is tabulated in Table 3. No slip boundary condition is used at the wall of the catalytic converter.

5.2. Governing equations

The governing equations are the equations of conservation of mass (both overall and individual species), momentum and energy, and are written as:

Continuity equation

$$\frac{\partial}{\partial t}(\rho)+\nabla.(\rho U)=0 \tag{1}$$

Where ρ is mixture density (kg/m^3), t is time (s), and U is mass averaged velocity (m/s).

Momentum equation

$$\frac{\partial}{\partial t}(\rho U)+\nabla.(\rho UU)=-\nabla p+\nabla.\tau+\rho B \tag{2}$$

Where p is pressure (Pa), τ is shear stress (N/m^2) and B is body force vector (m/s^2).

Energy equation

$$\frac{\partial}{\partial t}(\rho h)+\nabla.(\rho Uh)=-\nabla.q+\dot{S}_h \tag{3}$$

Where h is enthalpy of mixture (J/kg), q is heat flux (W/m^2) and $\dot{S}_h$ is volumetric heat generation rate (W/m^3).

Species balance equation

$$\frac{\partial}{\partial t}(\rho Y_k)+\nabla.(\rho UY_k)=-\nabla.J_k+\dot{S}_k \qquad k=1,2,....,N \tag{4}$$

Where Y_k is mass fraction of k_{th} species, J_k is diffusion mass fraction of k_{th} species and $\dot{S}_k$ is production rate of k_{th} species due to homogeneous reaction (kg m^{-3} s^{-1}).

5.3. Solution procedure

The governing equations were solved by using SIMPLE algorithm and employing the second order upwind scheme in the spatial direction. The under relaxation factors for the species was taken as 0.95 for the first 100 iteration and then increased to 1.0 for faster convergence in the remaining iterations. The inlet gas concentrations are determined by experiment that calculates the exhaust properties from an engine operating at different loads. These data includes gas temperature, mass fraction of O_2, N_2, HC, CO_2, CO, NO and NO_2 and total flow rate. The amount of ammonia and SO_2 gas in the engine exhaust gases is assumed to be zero.

Table 3 Composition of combustion gases at the inlet

Species	Mass Concentration
O_2	7470 ppm
N_2	80.026 %
HC	700 ppm
CO_2	17.904 %
CO	1.14 %
NO_2	600 ppm
NO	530 ppm

6. Results and discussion

6.1. Axial Flow Converters

Initially the grid independence test was performed to eliminate the errors due to coarseness of the grid; analysis has been carried for different number of cells. The CFD model was assessed using experimental measurements under steady state condition. The model's predictions under steady state conditions were compared with the experimental measurements. The feed gas conditions used in this case are listed in Table 3. The mass fraction of species is plotted as a function of position along the length of the catalytic converter from inlet to outlet. The figure depicts that the CFD model results are in good agreement with the experimental measurements.

Figures 4(a) and 4(b) shows contour plot of static pressure and temperature along the length of the converter respectively. Figure 4(a) depicts that static pressure reduces drastically when a combustion gas enters the substrate. The high pressure is located around the catalyst entrance and the centre line. Figure 5 show the velocity vector plot at surface y=0. It is shown that a large circulation zone is formed in the diffuser. When the flow enters the porous zone, it aligns with the channel direction. Figures 6(a), 7(a), 8(a) and 9(a) show the contour plot of mass fraction of CO, CO_2, HC and NO_x at the inlet gas temperature of 620 K. Figures 6(b), 7(b), 8(b) and 9(b) represent the plot of mass fraction of CO, CO_2, HC and NO_x respectively as a function of position.

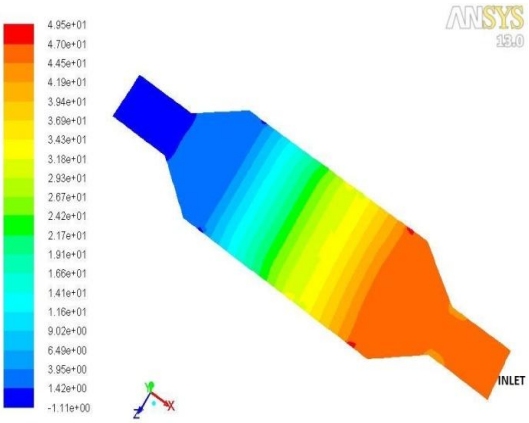

Fig. 4(a) Contour of Static pressure along the length of a catalytic converter

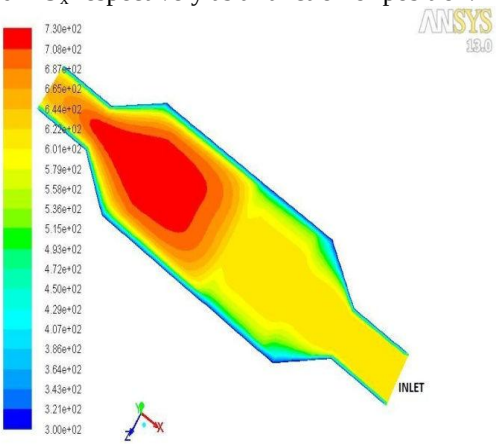

Fig. 4(b) Contour of Temperature along the length of a catalytic converter

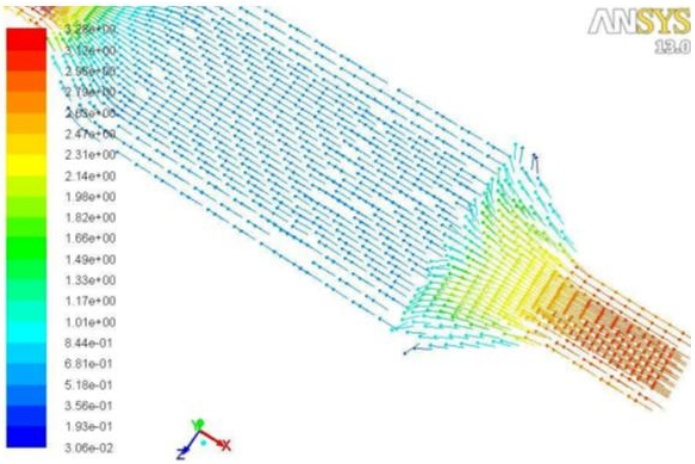

Fig. 5 velocity vectors along the length of catalytic converter

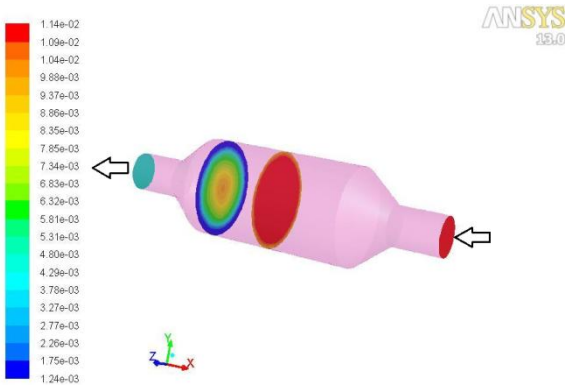

Fig. 6(a) Contour plot of mass fraction of CO

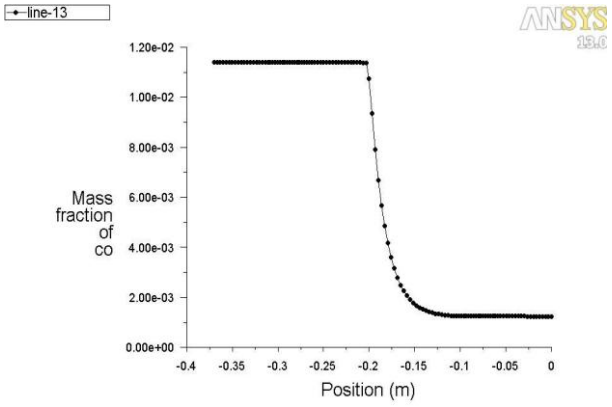

Fig. 6(b) Mass fraction of CO along the length of catalytic converter at 620K

Fig. 7(a) Contour plot of mass fraction of

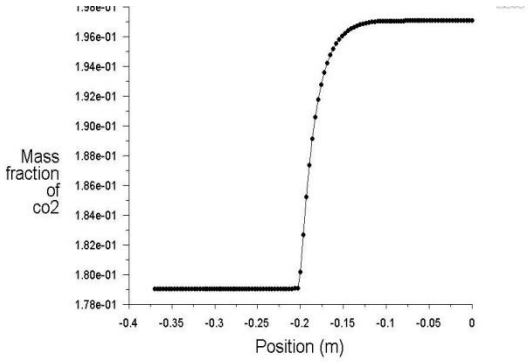

Fig. 7(b) Mass fraction of CO_2 along the length of catalytic converter at 620K

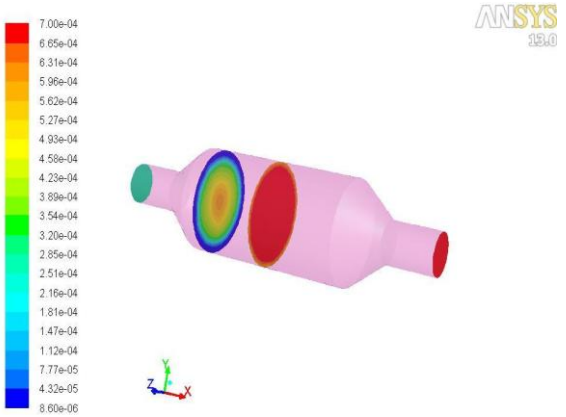

Fig. 8(a) Contour plot of mass fraction of

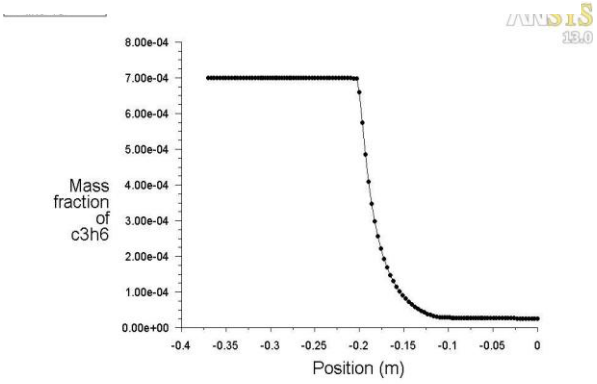

Fig. 8(b) Mass fraction of HC along the length of catalytic converter at 620K

Fig. 9(a) Contour plot of mass fraction of

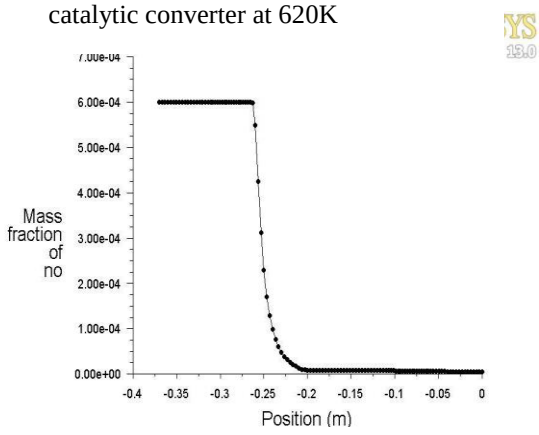

Fig. 9(b) Mass fraction of NO_x along the length of catalytic converter at 620K

The inlet gas temperature is varied from 500K to 700K. Figure depicts that the simulated results are in good agreement with the experimental measurements. There is a competition between CO, HC and O_2. In the temperature range between 500K and 700K, there is a slight increase of the calculated conversion efficiency of CO, accompanied by a slight decrease of conversion efficiency of HC. The under estimation of the HC conversion at 700K could be corrected by a turning of the kinetics parameters. The NOx is completely converted at 650K.

6.2. Radial Flow Converters

The model design is changed from axial to radial flow and the simulation is done on the radial flow model. Figure 10(a) shows the velocity vectors along the length of radial flow catalytic converter. Figure depicts that the radial flow creates turbulence on substrate entry after direction change of circa 90^0 and the slow gas speed at the substrate exit assuring low back pressure between this point and the outlet pipe. Figure 11 shows the plot of mass fraction of CO, CO_2, NO_x and HC along the diameter of radial flow catalytic converter. Figure depicts that the concentrations of CO, NO_x and HC is decreasing radially from the center to the wall of the converter and since CO is oxidized to CO_2 and HC is oxidized to CO_2 and H_2O, the concentration of CO_2 is increasing radially from the center to the wall of the converter. NO_x is reduced to nitrogen and oxygen.

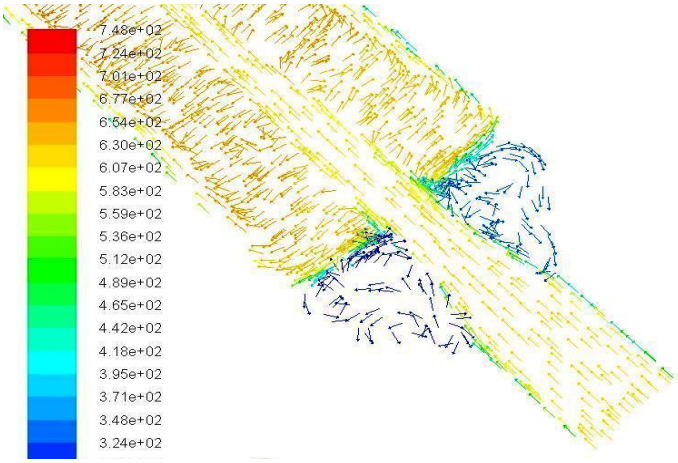

Fig. 10(a) Velocity Vectors (Radial flow)

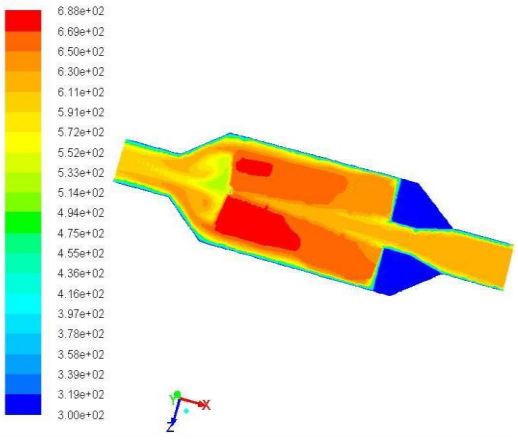

Fig. 10(b) Contours of Temperature along the length of converter (radial flow)

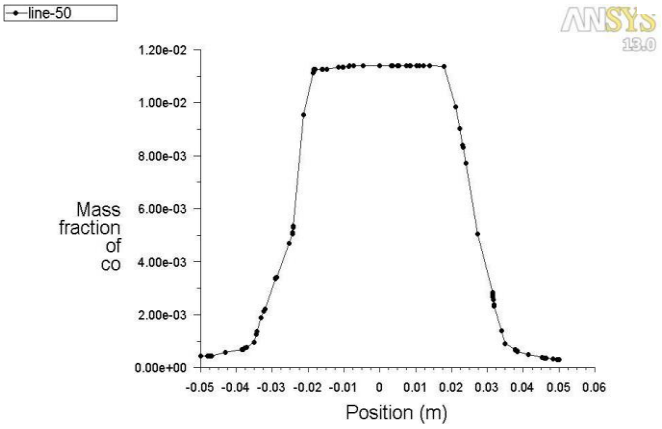

Fig. 11(a) Mass fraction of CO along the diameter of catalytic converter.

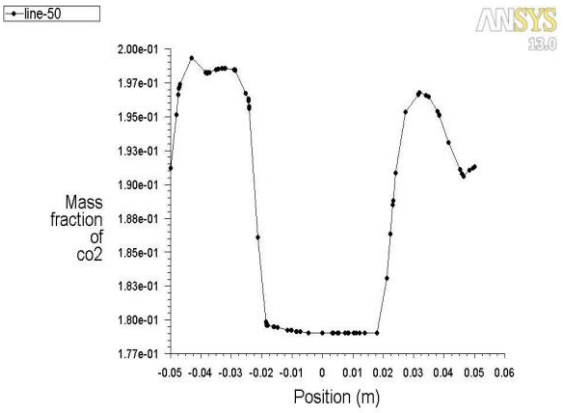

Fig. 11(b) Mass fraction of CO_2 along the diameter of catalytic converter.

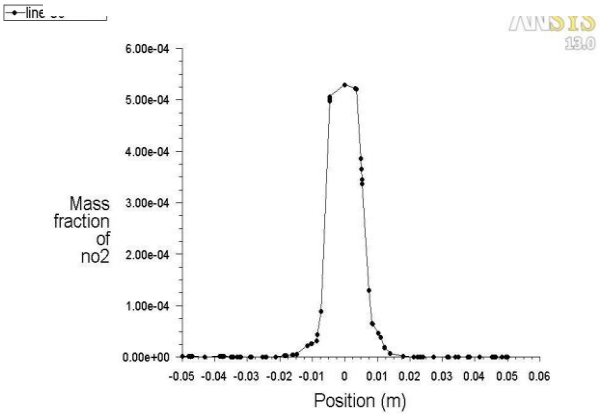

Fig. 11(c) Mass fraction of NOx along the diameter of catalytic converter.

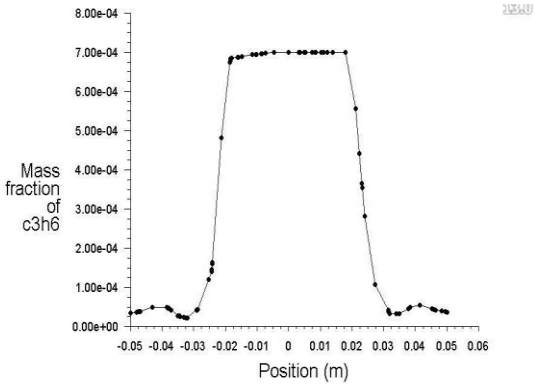

Fig. 11(d) Mass fraction of HC along the diameter of catalytic converter.

Table 4 Comparison of initial and final concentrations of species

Specie	Initial Concentration	Final Concentration Axial Flow	Final Concentration Radial Flow
CO	0.0114	0.001231	0.000443
CO_2	0.17904	0.19116	0.19585
HC	0.0007	5.39 e-5	4.53 e-5
NO	0.0006	3.48 e-6	9.28 e-7
NO_2	0.00053	3.08 e-6	7.89 e-7
O_2	0.00747	0.002711	3.66 e-4

Table 5 Comparison of conversion efficiencies between model predictions and experimental measurements

Efficiency %	CO	HC	NO_x
Experimental	87.54	91.43	97.92
Modal prediction Axial Flow	89.20	92.23	99.42
Model prediction Radial Flow	95.60	93.52	99.84

The initial and final concentrations of species are listed in Table 4. Comparison of pollutant conversion efficiencies as determined by the model and experimental measurements is shown in Table 5. The table clearly shows the adequacy of the CFD model in simulating the performance of three-way catalytic converter. There is a difference of less than five percent between the conversion efficiencies predicted by the CFD axial flow model and those determined experimentally. The result also shows that the conversion from axial to radial flow leads to increase in the conversion efficiency of the catalytic converter.

7. Conclusion

The 3D CFD modeling of a catalytic converter was developed in this paper. The proposed chemical reaction mechanism was able for reducing NO and NO_2 and oxidation of CO and HC. The experiment is carried out for the measurement of species at different loads. The simulated results show good agreement with the experimental measurements at steady-state condition. The model predicts the pollutant conversion efficiencies within five percent of the experimental measurements. The model also predicts that the conversion efficiency of catalytic converter increases as the flow changes its direction at the entry of the substrate through 90^0.

Acknowledgement

The support from project guide, Dr. V.R.Kalamkar, Sardar Patel College of engineering and IIT-Powai, Mumbai, is greatly appreciated.

Nomenclature

Symbols

B	body force vector (m/s^2)
h	enthalpy of mixture (J/kg)
J_k	diffusion mass flux of the *k*th species
p	pressure (Pa)
q	heat flux (W/m^2)
$\dot{S}_k$	production rate of *k*th species due to homogeneous reaction ($kg\ m^{-3}\ s^{-1}$)
$\dot{S}_h$	volumetric heat generation rate ($W\ m^{-3}$)
T	temperature (K)
U	mass averaged velocity (m/s)
Y_k	mass fraction of *k*th species

Greek

ρ	mixture density (kg m^{-3})
τ	shear stress (N/m^2)

Acronyms

CFD	Computational Fluid Dynamics
ICEM	Integrated Computer Engineering and Manufacturing
SIMPLE	Semi-Implicit Method for Pressure Linked Equations.

References

[1] Vardi J., Biller W. F., 1968, "Thermal behavior of an exhaust gas catalytic converter," Ind. Eng. Chem–Process Des Dev., 7(1):83–90.

[2] Kuo J. C., Morgan C. R., Lassen H. G., "Mathematical modeling of CO and HC catalytic converter systems," SAE paper 710289.

[3] Harned J. L., Montgomery D. L., "Comparison of catalyst substrate for catalytic converter systems," SAE paper 730561.

[4] Oh S. H., Cavendish J. C., 1982, "Transients of monolithic catalytic converters: response to step changes in feedstream temperature as related to controlling automobile emissions," Ind Eng Chem Res;21:29-37.

[5] Pattas K. N., Stamatelos A. M., Pistikopoulos P. K., Koltsakis G. C., Konstandinidis P. A., Volpi E., et al, 1994, "Transient modeling of 3-way catalytic converters," SAE paper 940934.

[6] Tischer, S., Correa, C. and Deutschmann, O., 2001, "Transient Three-Dimensional Simulations of a Catalytic Combustion Monolith Using Detailed Models for Heterogeneous and Homogeneous Reactions and Transport Phenomena," Catal. Today, 69, pp. 57-62.

[7] Koltsakis, G. C., and Stamatelos, A. M., 1997, "Catalytic Automotive Exhaust Aftertreatment," Prog. Energy Combust. Sci., 23, pp. 1-37.

[8] Lai, M. C., Lee, T., Kim, J. Y., Li, P., Chui, G. and Pakko, J. D., 1992, "Numerical and Experimental Characterization of Automotive Catalytic Converter Internal Flows," J. Fluids Struct., 6, pp. 451-470.

[9] Charles N. Satterfield, 1981, "Mass Transfer in Heterogeneous Catalysis," Robert E. Krieger Publishing Company, Inc.

[10] Otto, N. C. and LeGray, W. J., 1980, "Mathematical Models for Catalytic Converter Performance," SAE Paper No. 800841.

[11] FLUENT 6.1.18, FLUENT Inc.

[12] S. Siemund, D. Schweich, J. P. Leclerc and J. Villermaux, 1995, "Modelling Three-Way Monolithic Catalytic Converter: Comparison Between Simulation and Experimental Data," Catalysis and Automotive Pollution Control, III, Studies in Surface Science and Catalysis, Vol. 96.

[13] T.Shamim, S.Sengupta, A.A.Adamczyk, 2002, "A comprehensive model to predict three way catalytic converter performance," Journal of Engineering for Gas Turbines and Power, April 2002, Vol. 124 / 421.

[14] Ming Chen, Joe Aleixo, Shazam Williams & Thierry Leprince, "CFD modeling of three way catalytic converters with detailed catalytic surface reaction mechanism," DCL International Inc.

[15] Sandip Mazumder, "Modeling full scale monolith catalytic converters," Transactions of the ASME, 526 / Vol. 129, April 2007.

[16] Depcik C., 2003 "Modeling reacting gases and aftertreatment devices for internal combustion engines," PhD in mechanical engineering. Ann Arbor, Michiganr: The University of Michigan.

[17] Young L. C., Finlayson B. A., 1976, "Mathematical models of the monolithic catalytic converter: part II. Application to automobile exhaust," AIChE J, 22(2):343-53.

[18] Christopher Depcik, Dennis Assanis, 2005, "One-dimensional automotive catalyst modeling," Progress in Energy and Combustion Science 31, pp. 308-369.

[19] Hua Lun, Niu Xiaoweiy, Zhou Liangz, 2010, "CFD simulation of the effect of monolith wall thickness on the light off performance of a catalytic converter," International journal of chemical reactor engineering, Vol. 8.